

Spectroscopic and Microscopic Studies on the Mechanism of Mitochondrial Toxicity Induced by CdTe QDs Modified with Different Ligands

Lu Lai · Jian-Cheng Jin · Zi-Qiang Xu ·
Yu-Shu Ge · Feng-Lei Jiang · Yi Liu

Received: 7 December 2014 / Accepted: 24 February 2015 / Published online: 11 March 2015
© Springer Science+Business Media New York 2015

Abstract Quantum dots (QDs) are increasingly applied in sensing, drug delivery, biomedical imaging, electronics industries, etc. Consequently, it is urgently required to examine their potential threat to humans and the environment. In the present work, the toxicity of CdTe QDs with nearly identical maximum emission wavelength but modified with two different ligands (MPA and BSA) to mitochondria was investigated using flow cytometry, spectroscopic, and microscopic methods. The results showed that QDs induced mitochondrial permeability transition (MPT), which resulted in mitochondrial swelling, collapse of the membrane potential, inner membrane permeability to H^+ and K^+ , the increase of membrane fluidity, depression of respiration, alterations of ultrastructure, and the release of cytochrome *c*. Furthermore, the protective effects of CsA and EDTA confirmed QDs might be able to

induce MPT via a Ca^{2+} -dependent domain. However, the difference between the influence of CdTe QDs and that of Cd^{2+} on mitochondrial membrane fluidity indicated the release of Cd^{2+} was not the sole reason that QDs induced mitochondrial dysfunction, which might be related to the nanoscale effect of QDs. Compared with MPA-CdTe QDs, BSA-CdTe QDs had a greater effect on the mitochondrial swelling, membrane fluidity, and permeabilization to H^+ and K^+ by mitochondrial inner membrane, which was caused the fact that BSA was more lipophilic than MPA. This study provides an important basis for understanding the mechanism of the toxicity of CdTe QDs to mitochondria, and valuable information for safe use of QDs in the future.

Keywords Mitochondria · Quantum dots · Mitochondrial permeability transition · Apoptosis · Swelling

Electronic supplementary material The online version of this article (doi:10.1007/s00232-015-9785-x) contains supplementary material, which is available to authorized users.

L. Lai · J.-C. Jin · Z.-Q. Xu · Y.-S. Ge · F.-L. Jiang (✉) ·
Y. Liu (✉)

State Key Laboratory of Virology & Key Laboratory of Analytical Chemistry for Biology and Medicine (Ministry of Education), College of Chemistry and Molecule Sciences, Wuhan University, Wuhan 430072, People's Republic of China
e-mail: fljiang@whu.edu.cn

Y. Liu
e-mail: yiliu@whu.edu.cn

L. Lai
College of Chemistry and Environmental Engineering, Yangtze University, Jingzhou 434023, People's Republic of China

Y. Liu
College of Chemistry and Material Sciences, Hubei Engineering University, Xiaogan 432000, People's Republic of China

Abbreviations

HP	Hematoporphyrin
MPA	3-Mercaptopropionic acid
BSA	Bovine serum albumin
CsA	Cyclosporin A
QDs	Quantum dots
MPT	Mitochondrial permeability transition
ROS	Reactive oxygen species
CNTs	Carbon nanotubes

Introduction

Quantum dots are tiny particles, or “nanoparticles”, of a semiconductor material, traditionally chalcogenides (tellurides, selenides or sulfides) of metals like cadmium or zinc (CdTe or ZnS, for example), which range from 2 to

10 nm in diameter (about the width of 50 atoms). Because of their small size, quantum dots display unique optical and electrical properties that are different in character from those of the corresponding bulk material (Murray et al. 2000). The wavelength of these photon emissions depends not on the material from which the quantum dot is made, but its size (Ekimov and Onushchenko 1981). Quantum dots can therefore be “tuned” during production to emit any color of light desired (Leutwyler et al. 1996). Researchers have studied the applications of quantum dots in transistors, solar cells (Nozik 2002), LEDs (Leutwyler et al. 1996), and diode lasers (Narukawa et al. 1997). They have also investigated quantum dots as agents for medical imaging (Michalet et al. 2005) and as possible qubits in quantum computing (Loss and DiVincenzo 1998). To prevent potential threats originating from accidental exposure of quantum dots, their toxicity has been extensively studied at the levels of biological macromolecules (Atay et al. 2010; Vannoy and Leblanc 2010; Xiao et al. 2012), subcellular organelles (Li et al. 2011b), cell (Chibli et al. 2011; Clift et al. 2011b; Derfus et al. 2004; Hoshino et al. 2004; Lu et al. 2008; Neibert and Maysinger, 2012), protozoa (Werlin et al. 2011), and others (Donaldson et al. 2002; Lu et al. 2008; Mortensen et al. 2013; Yang et al. 2014).

The mitochondrion is a membrane-bound organelle found in most eukaryotic cells. Mitochondria range from 0.5 to 1.0 μm in diameter. These structures are sometimes described as “cellular power plants” because they generate most of the cell’s supply of ATP, used as a source of chemical energy (Henze and Martin 2003). In addition to supplying cellular energy, mitochondria are involved in the processes such as signaling, cell differentiation, cell growth, cell death, as well as the control of the cell cycle (McBride et al. 2006). Mitochondria have been implicated in several human diseases, including mitochondrial disorders and cardiac dysfunction, and may play a role in the aging process (Lesnefsky et al. 2001). Previous studies demonstrated that the consistent characteristics of apoptosis, produced by a variety of stimuli and in a number of different cell types, appear to indicate common pathways. The consistent observation of mitochondrial dysfunction prior to the nuclear changes associated with apoptotic cell death implies that it may be a critical regulator of the metabolic events involved in the apoptotic cascade (Deckwerth and Johnson 1993; Isenberg and Klaunig 2000). Subsequent evidence revealed only mitochondria undergoing the mitochondrial membrane permeability transition (MPT) are pro-apoptotic in this system (Zamzami et al. 1996). MPT is defined as an increase in the permeability of the mitochondrial membranes for molecules of less than 1500 Da in molecular weight (Bernardi et al. 1994). MPT results from the opening of a

mitochondrial permeability transition pore, also known as the MPT pore or MPTP. Induction of the permeability transition pore can lead to mitochondrial swelling and cell death through apoptosis or necrosis.

Recently, some studies showed that several types of nanoparticles, such as quantum dots (Lovrić et al. 2005), Ag (Stensberg et al. 2014; Teodoro et al. 2011), CNTs (Pulskamp et al. 2007), and TiO_2 (Freyre-Fonseca et al. 2011), can damage mitochondria by causing mitochondrial swelling or collapse of the mitochondrial membrane potential. Sun et al. indicated silica nanoparticles could enter the cells through different pathways and dispersed in cytoplasm and deposited inside mitochondria. Mitochondria were the major organelles for the cytotoxicity of silica nanoparticles exposure (Sun et al. 2011). Additionally, it has been reported that CdSe-core QD treatment of IMR-32 cells induced JNK activation and mitochondrial-dependent apoptotic processes (Chan et al. 2006). It is widely accepted that the release of heavy metal ion and generation of reactive oxygen species (ROS) caused by highly reactive atoms at the particle surface are important mechanisms in the mitochondrial effects of quantum dots. Thus far, most reported nanotoxicological studies have focused on mitochondria dysfunction in vitro cell-culture experiments. However, the evidences of a direct and immediate influence of QDs on mitochondrial inner membrane permeabilization, ultrastructure, and permeability transition are still less documented. Recently, Clift et al. investigated the uptake and intracellular fate of a series of different surface-coated QDs (Clift et al. 2011a). The results showed that $\text{NH}_2(\text{PEG})$ -QDs were located within the mitochondria of macrophages. Noteworthy, our group investigated the effects of CdTe QDs on the function of mitochondria isolated from rat liver, and first presented mitochondria as target of quantum dots toxicity (Li et al. 2011a). Consequently, it is urgently required to examine the mechanism of mitochondrial toxicity induced by CdTe QDs.

In order to stabilize nanoparticles, alleviate toxicity and target organs, quantum dots are usually coated with ligands or polymers, or functionalized with peptide sequences. Bovine serum albumin (BSA) is a serum albumin derived from cows. Reportedly, the presence of BSA greatly improved the biocompatibility of QDs at the level of cells. We wonder if BSA has the same effect at the level of organelle. In the present work, the toxicity of CdTe QDs coated with two different ligands (MPA and BSA) to mitochondria was investigated using flow cytometry, spectroscopic, and microscopic methods. Our study provides an important basis for understanding the mechanisms of CdTe QDs toxicity to mitochondria. The above features of QD-induced mitochondrial dysfunction will be useful for studies on the biological activities of QDs.

Experimental

Cells and Reagents

3-Mercaptopropionic acid (MPA, 99 %), CdCl₂ (99.99 %), NaBH₄ (99 %), tellurium powder (99.999 %, about 200 mesh), bovine serum albumin (BSA), hematoporphyrin (HP), and cyclosporin A (CsA) were obtained from Sigma-Aldrich and were used without further purification. All other reagents were of analytical reagent grade. Ultrapure water with 18.2 MΩ cm⁻¹ (Millipore Simplicity) was used in all syntheses.

Preparation and Characterization of CdTe QDs

Experimental details for preparation and characterization of QDs modified by MPA and BSA are described in the supplementary material. All the QDs suspensions were purified by dialysis against 1 × 10⁻² mol L⁻¹ PBS buffer, pH = 7.4 for 2 h. QDs concentrations were determined using the extinction coefficients.

Cell Culture and Cell Treatment

Human embryonic kidney cells (HEK293 cell) were cultured in Dulbecco's modified Eagle's medium (DMEM), supplemented with 10 % heat-inactivated fetal bovine serum (FBS), and antibiotics (100 mg/mL streptomycin and 100 U/mL penicillin) at 37 °C in the humidified atmosphere with 5 % CO₂. For flow cytometry, cells were cultured at a density of 3.0 × 10⁵ cells/well in 6-well plates (Corning Incorporated, Corning, NY, US). Cells were treated with QDs for 24 or 48 h before biochemical analysis and real-time live cell imaging.

Assessment of Cell Metabolic Activity

Colorimetric 3-(4,5-dimethylthiazol-2-yl)-2,5-diphenyl tetrazolium bromide (MTT) assays were performed to assess the metabolic activity of cells. The cells in culture medium were dispensed in 96-well plates (200 μL in each well containing 2 × 10⁴ cells per well). Then different concentrations of QDs were added to each well. After 48 h treatment medium was removed and replaced by phosphate buffer (180 μL/well). To each well 20 μL stock MTT (5 mg/mL) was added, and cells were then incubated for 4 h at 37 °C. Medium was removed, and cells were lysed with dimethylsulfoxide. Absorbance was measured at 490 nm using a microplate reader (Elx800, BioTek, USA). Relative cell viability was calculated as a percentage of the control group, to which QDs had not been added.

Isolation of Mitochondria

Liver mitochondria from Wistar rats (150–200 g) were isolated according to standard differential centrifugation procedures. In brief, the liver tissue was homogenized in medium A, containing 250 mM sucrose, 2 mM HEPES, 0.1 mM EDTA, and 0.1 % fatty acid-free BSA (pH 7.4). The protein concentration of mitochondria was determined by the biuret method using BSA as the standard. The respiratory control ratio (RCR) was measured by a Clark electrode (Oxygraph, Hansatech, UK). Only when the respiratory control ratio value exceeded 3, the mitochondrial suspensions were used.

Evaluation of Mitochondrial Membrane Potential ($\Delta\psi_m$)

For quantitative analysis of $\Delta\psi_m$, QDs-treated HEK293 cells were also rinsed twice with PBS, trypsinized, and then stained with JC-1. JC-1 is a lipophilic probe which potential-dependently accumulated in mitochondria and its fluorescence emission shifts from red (~590 nm, J-aggregates) to green (~525 nm, J-monomers) when mitochondrial membrane potential decreases. The fluorescence of J-aggregates in healthy cells was quantified on PE detector, and green JC-1 monomers in apoptotic cells were quantified on FITC detector of flow cytometer (FACSAria™ III, Becton–Dickinson, USA). For statistical significance, at least 10,000 cells were analyzed in each sample. Confocal micrographs of HEK293 cells stained with JC-1 were acquired with Eclipse C1-si laser scanning confocal microscope system (Nikon).

Determination of Mitochondrial Swelling

Mitochondrial swelling was measured by monitoring the decrease of absorbance at 600 nm over 7.5 min at room temperature (Bernardi et al. 1992). Mitochondria (0.25 mg/mL) were suspended in 2 mL medium B (200 mM sucrose, 10 mM Tris-MOPS, 20 μM EGTA-Tris, 5 mM succinate, 2 μM rotenone, and 3 μg/mL oligomycin, pH 7.4) and incubated with different concentrations of QDs. Spectra were recorded at room temperature on a UNICO (Dayton, NJ) 4802 double beam spectrophotometer equipped with 1.0 cm quartz cells.

Measurement of H⁺ and K⁺ Inner Membrane Permeabilization

Mitochondrial inner membrane permeabilization to H⁺ or K⁺ was detected, respectively, by passive osmotic swelling of mitochondria suspended in potassium acetate and potassium nitrate medium (Fernandes et al. 2006). The

potassium acetate medium contained 135 mM potassium acetate, 5 mM HEPES, 0.1 mM EGTA, 0.2 mM EDTA, 2 μ M rotenone, and 1 μ g/mL valinomycin (pH 7.1), while the potassium nitrate medium contained 135 mM KNO₃, 5 mM HEPES, 0.1 mM EGTA, 0.2 mM EDTA, and 2 μ M rotenone (pH 7.1).

Assessment of Membrane Fluidity

Mitochondrial membrane fluidity was measured by the fluorescence anisotropy changes of HP-labeled mitochondria (Ricchelli et al. 2005). The HP solution was prepared in absolute ethanol and injected into stirred mitochondrial suspensions (0.25 mg/mL, in medium B) with a final concentration of 3 μ M. Fluorescence anisotropic (r) values were recorded at 626 nm ($\lambda_{\text{ex}} = 520$ nm) by measurements of I_{\parallel} and I_{\perp} , i.e., the fluorescence intensities polarized parallel and perpendicular, respectively, to the vertical polarization plane of the excitation beam. The anisotropy, r , is defined by the following equation:

$$r = \frac{I_{\parallel} - GI_{\perp}}{I_{\parallel} + 2GI_{\perp}},$$

where $G = I_{\perp}/I_{\parallel}$, G is the correction factor for instrumental artifacts.

Measurement of Mitochondrial Respiratory Rate

Respiratory rate was monitored by a Clark oxygen electrode and the Oxygraph software from Hansatech, UK.

Transmission Electron Microscopy of Cell and Mitochondria

Cells under various experimental conditions were fixed for 30 min at 4 °C using glutaraldehyde at a final concentration of 2.5 % in 0.1 M cacodylate buffer, then postfixed with 1 % osmium tetroxide and dehydrated (Petronilli et al. 2009). Observations were performed on a JEM-100CX transmission electron microscope (JEOL, Peabody, MA).

Measurement of Cytochrome C

To confirm apoptosis caused by QDs, the release of cytochrome *c* from mitochondria was detected by Cyt-C ELISA Kit (Shanghai Hua Yi Bio Technology Co. Ltd, China) according to manufacturer's protocol.

Statistical Analysis

All the experiments were performed using four independent experiments with different mitochondrial preparations. The values are expressed as mean \pm SE. Means were

compared using ANOVA (paired t test). Statistical significance was set as $P < 0.05$.

Results

Characterization of CdTe QDs

The images of CdTe QDs water dispersion under room light (left) and UV lamp (right) radiation are shown in Figure S1. Figure S2a, b show the UV-visible (UV-Vis) absorption (A) and photoluminescence (B) spectra of QDs at room temperature. All samples exhibit a well-resolved first electronic transition absorption maximum, indicating a sufficiently narrow size distribution. The line width of the fluorescence spectrum is narrow, which also suggest that the as-prepared QDs are nearly monodispersed and homogeneous (Zheng et al. 2007). Figure S3 reveals the powder X-ray diffraction (XRD) patterns for the precipitated fractions of CdTe QDs. These QDs exhibited the cubic (zinc blende) structure which was also the dominant crystal phase of bulk CdTe. The X-ray photoelectron spectra (XPS) of CdTe QDs are shown in Figure S4. The overview TEM image (Fig. 1a) presents well-separated nanocrystals with mean size of ~ 4 nm. A high-resolution TEM image (Fig. 1b) of the MPA-capped CdTe QDs shows crystalline nanoparticles with distinctly resolved lattice fringes.

Cytotoxicity of MPA-CdTe and BSA-CdTe QDs

The cytotoxicity of QDs was evaluated by the effect on the cellular metabolic viability through MTT assay. As shown in Fig. 2, MPA-CdTe QDs were highly toxic for HEK293 cells. On the contrary, the presence of BSA greatly improved the biocompatibility of QDs.

Effects of QDs on Mitochondrial Membrane Potential ($\Delta\psi_m$)

Mitochondrial permeability transition is an important step in the induction of cellular apoptosis. During this process, the electrochemical gradient across the mitochondrial membrane collapses. JC-1, a unique cationic dye (5,5',6,6'-tetrachloro-1,1',3,3'-tetraethylbenzimidazolylcarbocyanine iodide), is widely used to signal the loss of mitochondrial membrane potential. In healthy cells, the dye stains the mitochondria bright red. In apoptotic cells, the mitochondrial membrane potential collapses, and the JC-1 cannot accumulate within the mitochondria. In these cells, JC-1 remains in the cytoplasm in a green fluorescent monomeric form (Smiley et al. 1991). Consequently, mitochondrial depolarization is indicated by a decrease in the red/green

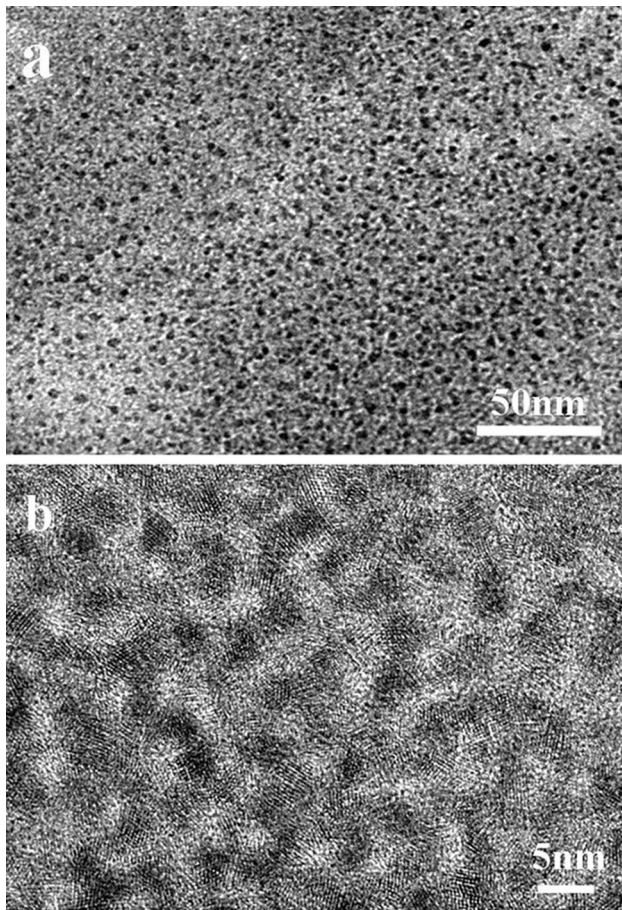


Fig. 1 TEM overview (a) and HRTEM image (b) of MPA-CdTe QDs

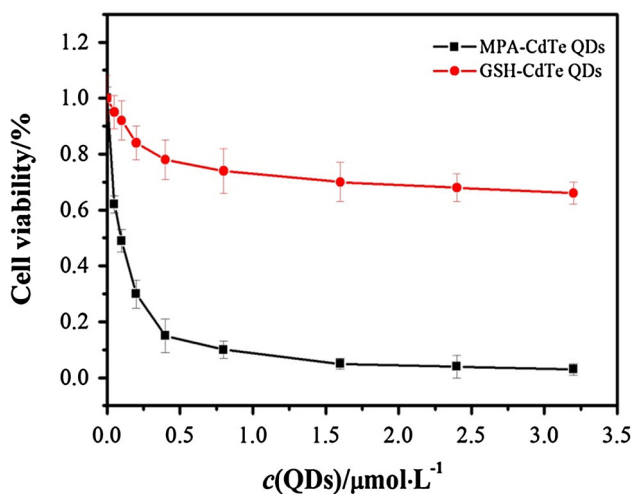


Fig. 2 Effects of MPA-CdTe and GSH-CdTe QDs on cell viability determined by MTT assay. HEK293 cells were incubated with different doses of MPA-CdTe and GSH-CdTe for 48 h. Error bars represent standard error of the mean (Color figure online)

fluorescence intensity ratio. Figure 3 shows the effect of MPA-CdTe QDs on mitochondrial membrane potential determined by flow cytometry. Collapse of the mitochondrial $\Delta\psi_m$ is demonstrated by an increase in the number of cells falling into P2 gate corresponding to a loss of red fluorescence, indicative of the onset of apoptosis or other $\Delta\psi_m$ depolarizing event. Percentage of HEK293 cells in P2 gate determined by JC-1 staining are listed in Table S1. MPA-CdTe QDs cause a pronounced reduction of $\Delta\psi_m$, as the percentage of unhealthy HEK293 cells with low $\Delta\psi_m$ were remarkably increased from 6.9 to 43.5 in the presence of 200 nM CdTe QDs. These results are also verified with the confocal micrographs of HEK293 cells stained with JC-1 (Fig. 4). Non-apoptotic cells exhibit orange-red stained mitochondria. When incubated with 50 nmol L⁻¹ MPA-CdTe QDs for 48 h, HEK293 cells contain less orange-red fluorescing J-aggregate and appear mostly green.

QDs Induce Mitochondrial Swelling

Mitochondrial swelling and collapse of the transmembrane potential are the direct results of MPT pore opening (Liu et al. 2011). In order to evaluate the effect of QDs on MPT, we examined whether QDs caused mitochondrial swelling. As shown in Fig. 5a, MPA-CdTe QDs induced mitochondrial swelling with a dose-dependent effect. Figure 5b shows the effect of Cd²⁺ and QDs modified with different surface ligands on mitochondrial swelling. In this experiment, the MPA-QDs concentration was fixed at 4 μmol L⁻¹. The ICP-AES results showed that 4 μmol L⁻¹ MPA-CdTe QDs solution used in this work contains an average of 320 μmol L⁻¹ Cd²⁺. Thus, the CdCl₂ concentration was set at 320 μmol L⁻¹. As shown in Fig. 5b, the Cd²⁺ has the greatest effect on the mitochondrial swelling and followed by BSA-CdTe QDs, the effect of MPA-CdTe QDs on the mitochondrial swelling is the weakest.

To better show the cytotoxic morphological changes of mitochondria induced by CdTe QDs, the ultrastructure of HEK 293 cells treated with or without CdTe QDs were examined by transmission electron microscopy (Fig. 6). The addition of MPA-CdTe QDs caused mitochondrial swelling with a large intermembrane space, clustering of the cristae, and expansion of the volume.

Permeabilization of Mitochondrial Inner Membrane to H⁺ and K⁺ Induced by QDs

The effects of QDs on permeabilization of mitochondrial inner membrane to H⁺ and K⁺ were evaluated by the

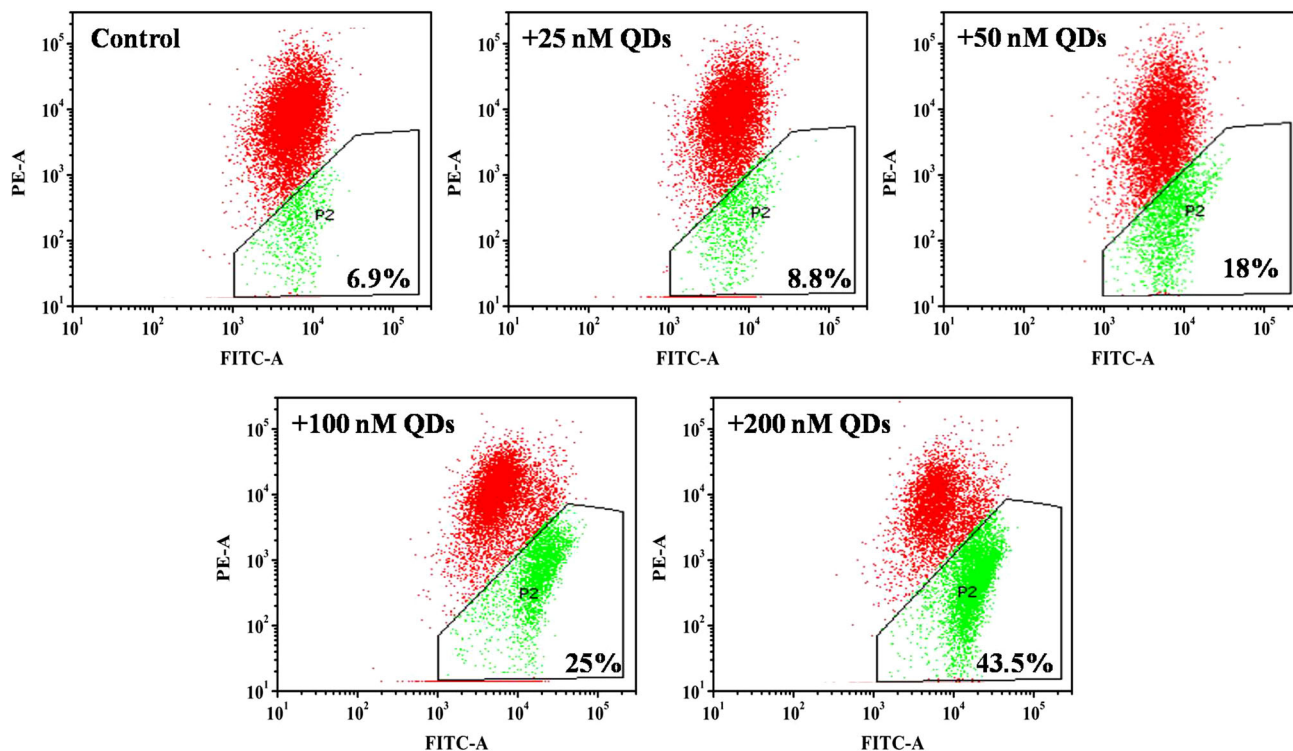


Fig. 3 Effects of MPA-CdTe QDs on mitochondrial membrane potential. HEK293 cells were incubated with different doses of MPA-CdTe QDs (0, 25, 50, 100, and 200 $\text{nmol}\cdot\text{L}^{-1}$) for 24 h, and then stained with JC-1. The *red* fluorescence of J-aggregates in healthy cells was quantified on PE detector, and *green* JC-1 monomers in apoptotic cells were quantified on FITC detector of flow cytometer.

Collapse of the mitochondrial $\Delta\Psi_m$ was demonstrated by an increase in the number of cells falling into P2 gate corresponding to a loss of *red* fluorescence. Records are representative of four experiments obtained from different mitochondrial preparations (Color figure online)

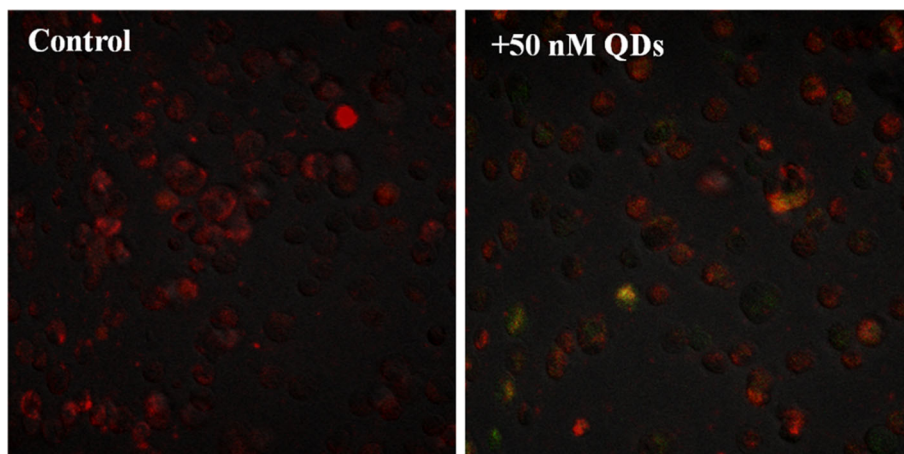


Fig. 4 Confocal micrographs of HEK293 cells stained with JC-1. HEK293 cells were incubated with MPA-CdTe QDs for 48 h. HEK293 cells were incubated with MPA-CdTe QDs (QDs) = 50 $\text{nmol}\cdot\text{L}^{-1}$. Confocal micrographs of HEK293 cells stained with JC-1 were acquired with Eclipse C1-si laser scanning confocal microscope system. Non-apoptotic cells exhibited *orange-*

red stained mitochondria. When incubated with 50 $\text{nmol}\cdot\text{L}^{-1}$ MPA-CdTe QDs for 48 h, HEK293 cells contained less *orange-red* fluorescing J-aggregate and appeared mostly *green*. Records are representative of four experiments obtained from different mitochondrial preparations

swelling of non-respiring mitochondria suspended in potassium acetate and potassium nitrate media, respectively (Liu et al. 2011). HAc can cross the mitochondrial inner membrane, and then enter into the mitochondrial

matrix, dissociate to the acetate anion and H^+ , producing a proton gradient. A valinomycin-dependent swelling only occurs if the proton gradient is dissipated (Bernardi et al. 1992). Thus, the effects of QDs on permeabilization of

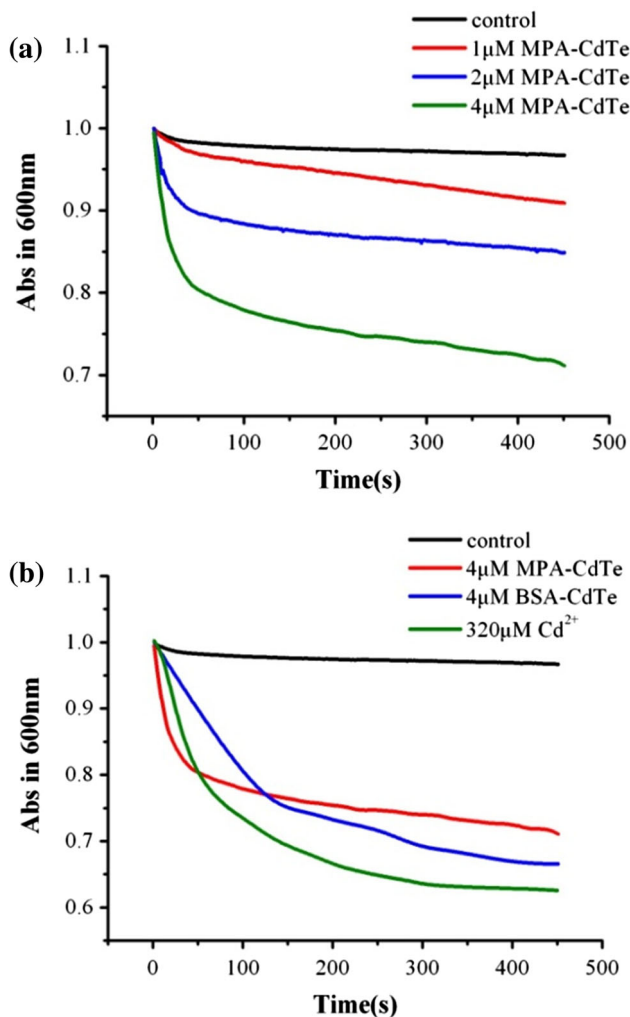


Fig. 5 QDs induced mitochondrial swelling. Mitochondrial swelling was measured by monitoring the decrease of absorbance at 600 nm at room temperature. Isolated mitochondria (0.25 mg/mL) were suspended in 2 mL of buffer containing 200 mM sucrose, 10 mM Tris-MOPS, 20 μM EGTA-Tris, 5 mM succinate, 2 μM rotenone, and 3 μg/mL oligomycin (pH 7.4), and incubated with different concentrations of QDs. **a** Mitochondria followed by addition of MPA-CdTe QDs: 0, 1, 2, and 4 μmol L⁻¹. MPA-CdTe QDs induced mitochondrial swelling with a dose-dependent effect. **b** Mitochondria followed by addition of 0, 4 μmol L⁻¹ MPA-CdTe, 4 μmol L⁻¹ BSA-CdTe QDs, and 320 μmol L⁻¹ Cd²⁺. The ICP-AES results showed that the 4 μmol L⁻¹ MPA-CdTe QDs solution used in this work contains an average of 320 μmol L⁻¹ Cd²⁺. The Cd²⁺ had the greatest effect on the mitochondrial swelling and followed by BSA-CdTe QDs, the effect of MPA-CdTe QDs on the mitochondrial swelling was the weakest. Records are representative of four experiments obtained from different mitochondrial preparations

mitochondrial inner membrane to H⁺ were evaluated according to the decrease in absorbance at 600 nm (A₆₀₀). Figure 7a shows that the untreated mitochondria undergo a little swelling in KAc media. The swelling may represent that H⁺ permeates across the inner membrane due to mitochondrial respiration in normal condition. In presence of QDs, the permeabilization of mitochondrial inner

membrane to H⁺ significantly increased as compared with untreated mitochondria, representing large proton conductance induced by QDs across the inner membrane. Furthermore, MPA-CdTe QDs induced permeabilization of mitochondrial inner membrane to H⁺ in a dose-dependent manner. Figure 7b shows the effect of Cd²⁺ and QDs modified with different surface ligands on permeabilization of mitochondrial inner membrane to H⁺. The Cd²⁺ had the greatest effect on the permeabilization of mitochondrial inner membrane and followed by BSA-CdTe QDs, the effect of MPA-CdTe QDs on the permeabilization of mitochondrial inner membrane was the weakest.

The ability of QDs to permeabilize mitochondrial inner membrane to K⁺ was tested by swelling of non-respiring mitochondria suspended in KNO₃ (Liu et al. 2011). Mitochondrial inner membrane freely permeabilizes nitrate, but swelling is observed only in conditions of K⁺ permeabilization. Addition of 1 μM MPA-CdTe QDs leads to obvious conductance of mitochondrial inner membrane, as detected by the increase of swelling (Fig. 8a). Moreover, MPA-CdTe QDs enhance the K⁺ conductance of the inner membrane with a dose-dependent effect. Figure 8b shows the effect of Cd²⁺ and QDs modified with different surface ligands on permeabilization of mitochondrial inner membrane to K⁺. The Cd²⁺ had the greatest effect on the permeabilization of mitochondrial inner membrane and followed by BSA-CdTe QDs, the effect of MPA-CdTe QDs on the permeabilization of mitochondrial inner membrane was the weakest.

The Effect of QDs on Membrane Fluidity

Recent studies have reported that induction of MPT in rat liver mitochondria was accompanied by fluidity changes of mitochondrial membranes (Ricchelli et al. 2005). The membrane fluidity changes can be evaluated by the changes of fluorescence anisotropy (*r*) of a mitochondria-bound dye (hematoporphyrin, HP). HP accumulates main in polar, solvent-accessible regions of the lipid bilayer, and protein regions of the inner membrane (Ricchelli et al. 1999). When HP is excited with polarized light, the resulting fluorescence is also polarized. Since the main cause of fluorescence depolarization is rotational diffusion of the fluorophore during the excited lifetime, fluorescence polarization measurements can be used to determine the rotational mobility of the fluorophore, which reflects the fluidity of the membrane. A high polarization value indicates low membrane fluidity or high structural order.

As shown in Fig. 9a, the HP anisotropy was continuously monitored. The addition of QDs caused an obvious decrease of the anisotropy of HP, which can be attributed to the increase of Brownian motion or energy transfer between identical chromophores. The results also

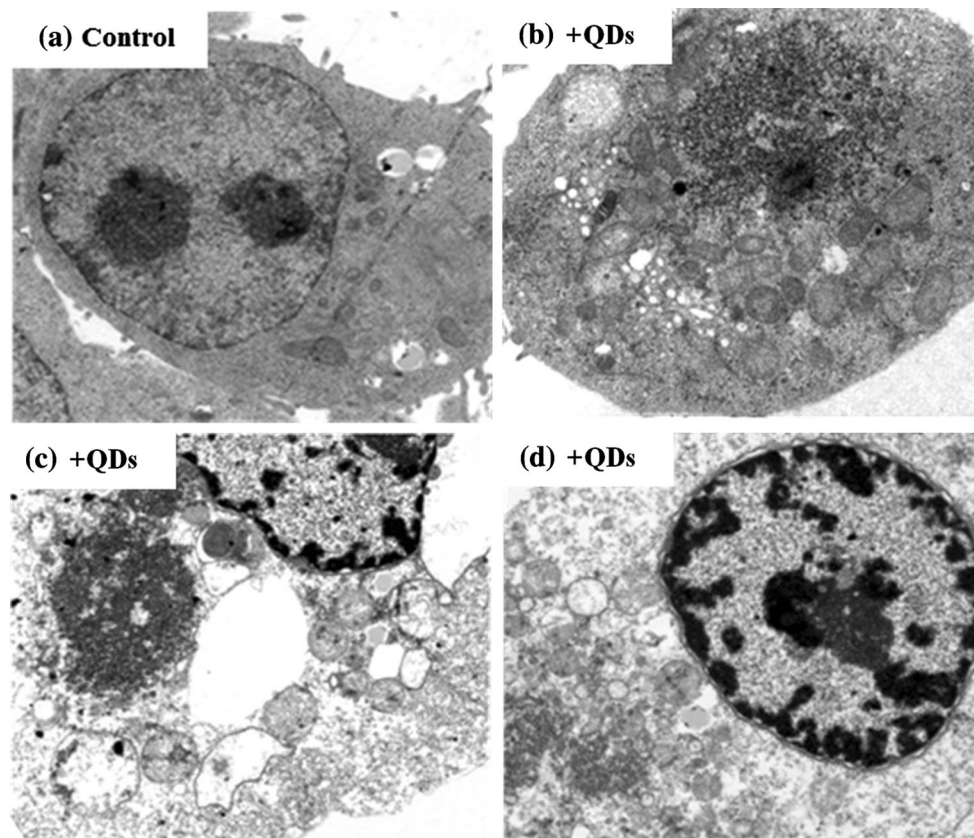


Fig. 6 Effects of MPA-CdTe QDs on the ultrastructural morphology of HEK293 cells by transmission electron microscopy. HEK293 cells were incubated in the absence (a) and presence of MPA-CdTe QDs (b, c, d) for 48 h. (QDs) = $50 \text{ nmol}\cdot\text{L}^{-1}$. Cells under various experimental conditions were fixed for 30 min at 4°C using

glutaraldehyde at a final concentration of 2.5 % in 0.1 M cacodylate buffer, and then postfixed with 1 % osmium tetroxide and dehydrated. The addition of MPA-CdTe QDs caused mitochondrial swelling with a large intermembrane space, clustering of the cristae, and expansion of the volume

demonstrate that MPA-CdTe QDs affected the fluidity of mitochondrial membranes in a concentration-dependent manner. Since the anisotropic changes of HP reflect the conformational variation of HP-binding regions on the mitochondrial membrane, the result indicates that the mitochondrial membrane structure is strongly disturbed. In addition, Fig. 9b shows the effect of Cd^{2+} and QDs modified with different surface ligands on mitochondrial membrane fluidity. The results suggest that the addition of Cd^{2+} (final concentration $32 \mu\text{M}$) cause an obvious increase of the anisotropy of HP, whereas MPA-CdTe QDs and BSA-CdTe QDs induce the obvious decrease of the anisotropy of HP. Therefore, the mechanism of the interaction of QDs with mitochondrial membrane is significantly different from that of Cd^{2+} .

Effects of QDs on Mitochondrial Respiratory Rate

Figure 10 shows the effects of MPA-CdTe QDs and BSA-CdTe QDs on the mitochondrial respiratory rate. In the control group, the high respiratory rate at state 3 indicates an intact respiratory chain and ATP synthesis.

Meanwhile, the low respiratory rate at state 4 suggests an intact mitochondrial inner membrane (Li et al. 2012). When exposed to QDs, the respiratory rates at state 3 and state 4 significantly decrease with the increase of the QDs concentration. This demonstrates that the addition of CdTe QDs inhibits the mitochondrial respiratory chain.

Release of Cytochrome *c* Induced by QDs

Cytochrome *c* is widely believed to be localized solely in the mitochondrial intermembrane space under normal physiological conditions. The release of cytochrome *c* from mitochondria to the cytosol, where it activates the caspase family of proteases, the primary trigger leading to the onset of apoptosis (Kobayashi et al. 2003). To confirm that QDs induced apoptosis, the release of cytochrome *c* was detected. As shown in Fig. 11, the addition of QDs promoted the release of cytochrome *c*, suggesting QDs can cause apoptosis. Moreover, the release of cytochrome *c* induced by MPA-CdTe QDs was more obvious compared with BSA-CdTe QDs.

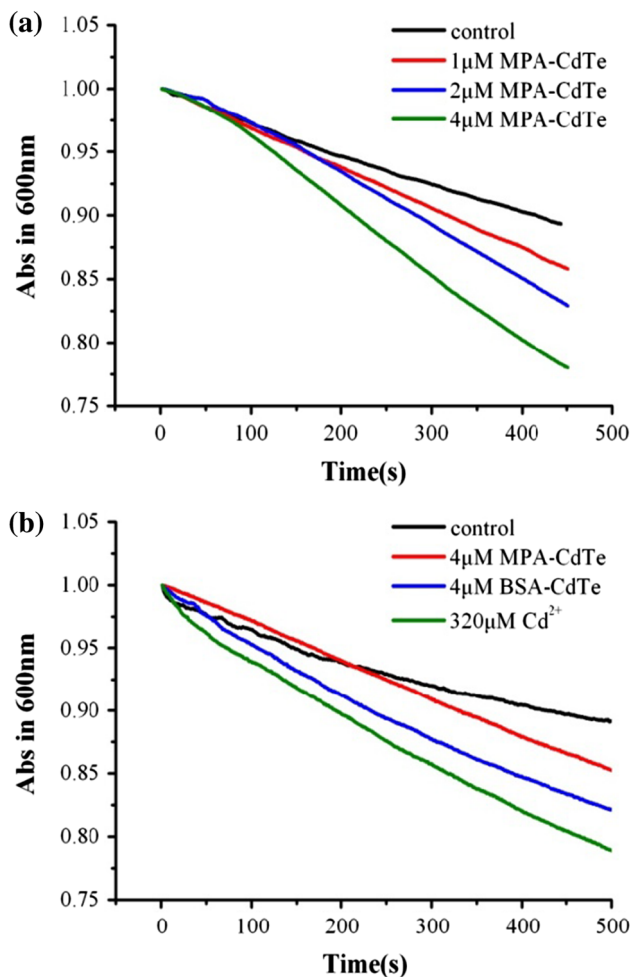


Fig. 7 Effects of QDs on the permeabilization to H^+ by mitochondrial inner membrane. Mitochondrial inner membrane permeabilization to H^+ was detected by passive osmotic swelling of mitochondria suspended in potassium acetate medium. The potassium acetate medium contained 135 mM potassium acetate, 5 mM HEPES, 0.1 mM EGTA, 0.2 mM EDTA, 2 μ M rotenone, and 1 μ g/mL valinomycin (pH 7.1). **a** Mitochondria followed by addition of MPA-CdTe QDs: 0, 1, 2, and 4 μ mol L^{-1} . **b** Mitochondria followed by addition of 0, 4 μ mol L^{-1} MPA-CdTe, 4 μ mol L^{-1} BSA-CdTe QDs, and 320 μ mol L^{-1} Cd^{2+} . The traces are typical recordings representative of four experiments obtained from different mitochondrial preparations

Interaction Sites of QDs on Mitochondria

To confirm the interaction sites of QDs on mitochondria, the effects of CsA and EDTA on mitochondrial swelling were detected. Although the structure of MPT pore, a protein channel, has not yet been identified, CsA is considered as a well-established inhibitor of the MPT pore. The inhibition by CsA is used to identify the characteristics of the MPT (Halestrap et al. 1997). As shown in Fig. 12, at the concentration of 0.1 mM, CsA notably inhibits the swelling of mitochondria, thus

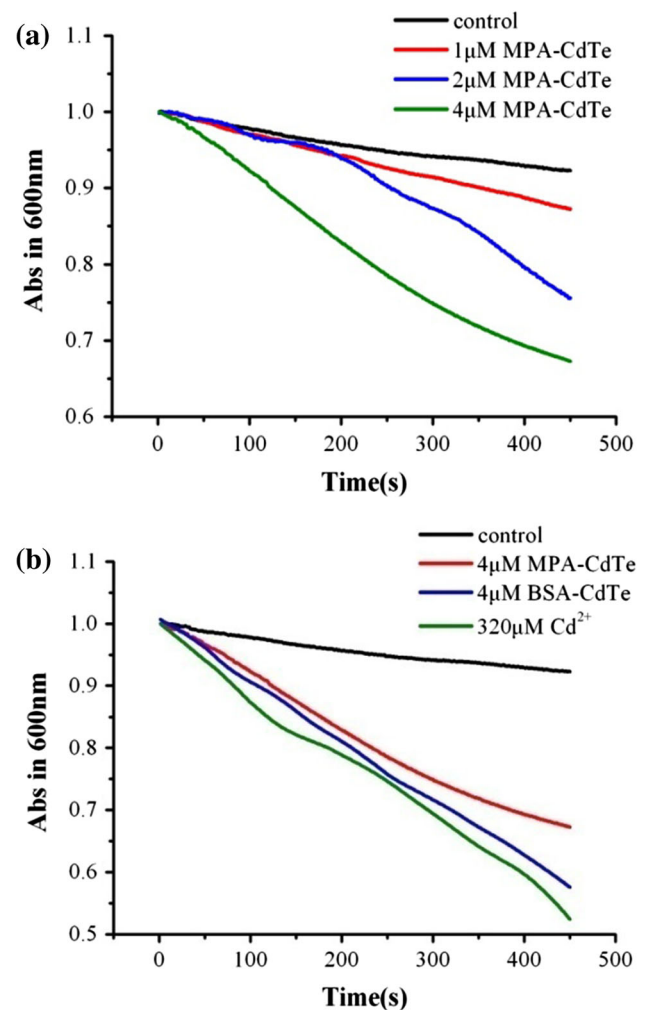


Fig. 8 Effects of QDs on the permeabilization to K^+ by mitochondrial inner membrane. Mitochondrial inner membrane permeabilization to K^+ was detected by passive osmotic swelling of mitochondria suspended in potassium nitrate medium. The potassium nitrate medium contained 135 mM KNO_3 , 5 mM HEPES, 0.1 mM EGTA, 0.2 mM EDTA, and 2 μ M rotenone (pH 7.1). **a** Mitochondria followed by addition of MPA-CdTe QDs: 0, 1, 2, and 4 μ mol L^{-1} . **b** Mitochondria followed by addition of 0, 4 μ mol L^{-1} MPA-CdTe QDs, 4 μ mol L^{-1} BSA-CdTe QDs, and 320 μ mol L^{-1} Cd^{2+} . The traces are typical recordings representative of four experiments obtained from different mitochondrial preparations

identifying the existence of MPT induced by MPA-CdTe QDs.

Previous studies indicated that the toxicity of CdTe QDs came from the release of Cd^{2+} . EDTA is mainly used to sequester metal ions in aqueous solution, and therefore inhibits the toxicity of Cd^{2+} . Further, it is known that mitochondria are able to reseal and fully recover energy-linked functions after the removal of calcium by chelation of EDTA (Zhang et al. 2011). We conducted a similar experiment with the addition of EDTA into the medium. As shown in Fig. 12, the mitochondrial swelling was obviously relieved by EDTA.

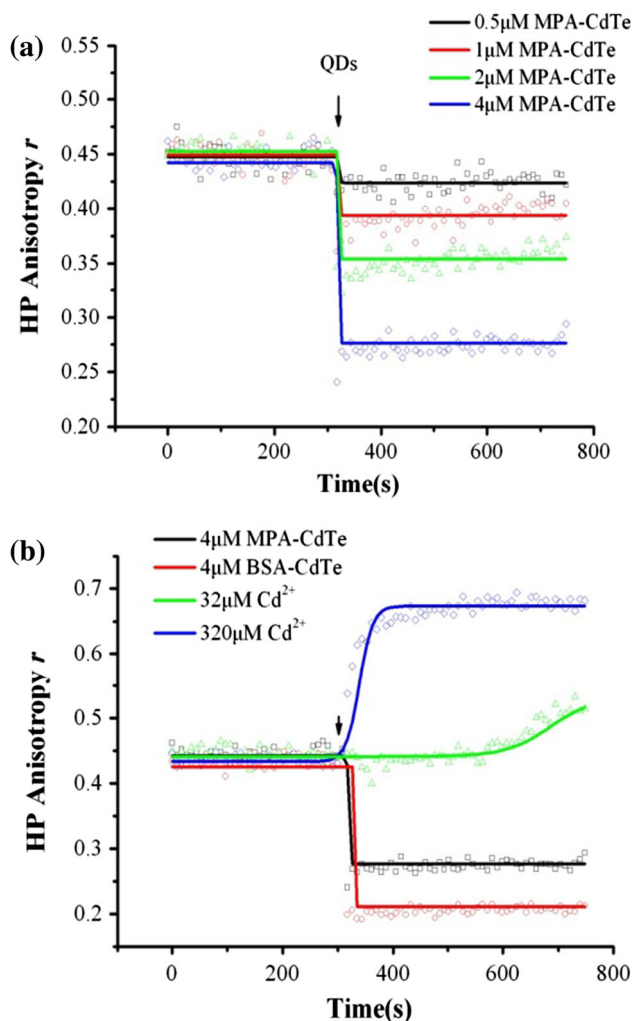


Fig. 9 Effects of QDs on the anisotropy changes of HP-labeled mitochondria. Isolated mitochondria (0.25 mg/mL) were suspended in 3 mL of buffer containing 200 mM sucrose, 10 mM Tris-MOPS, 20 μM EGTA-Tris, 5 mM succinate, 2 μM rotenone, and 3 $\mu\text{g/mL}$ oligomycin (pH7.4). The HP solution was prepared in absolute ethanol and injected into stirred mitochondrial suspensions with a final concentration of 3 μM . A high anisotropy value indicates low membrane fluidity or high structural order. **a** Mitochondria followed by addition of MPA-CdTe QDs: 0.5, 1, 2, and 4 $\mu\text{mol L}^{-1}$. The addition of QDs caused an obvious decrease of the anisotropy of HP in a concentration-dependent manner. **b** Mitochondria followed by addition of 4 $\mu\text{mol L}^{-1}$ MPA-CdTe QDs, 4 $\mu\text{mol L}^{-1}$ BSA-CdTe QDs, 32 $\mu\text{mol L}^{-1}$ Cd^{2+} , and 320 $\mu\text{mol L}^{-1}$ Cd^{2+} . The addition of Cd^{2+} (final concentration 32 or 320 μM) caused an obvious increase of the anisotropy of HP, whereas MPA-CdTe QDs and BSA-CdTe QDs induced the obvious decrease of the anisotropy of HP. The traces are typical recordings representative of four experiments obtained from different mitochondrial preparations

Discussion

The aim of this work is to investigate the interaction between different ligand-coated QDs and mitochondria. Previous studies in our group have suggested that QDs can

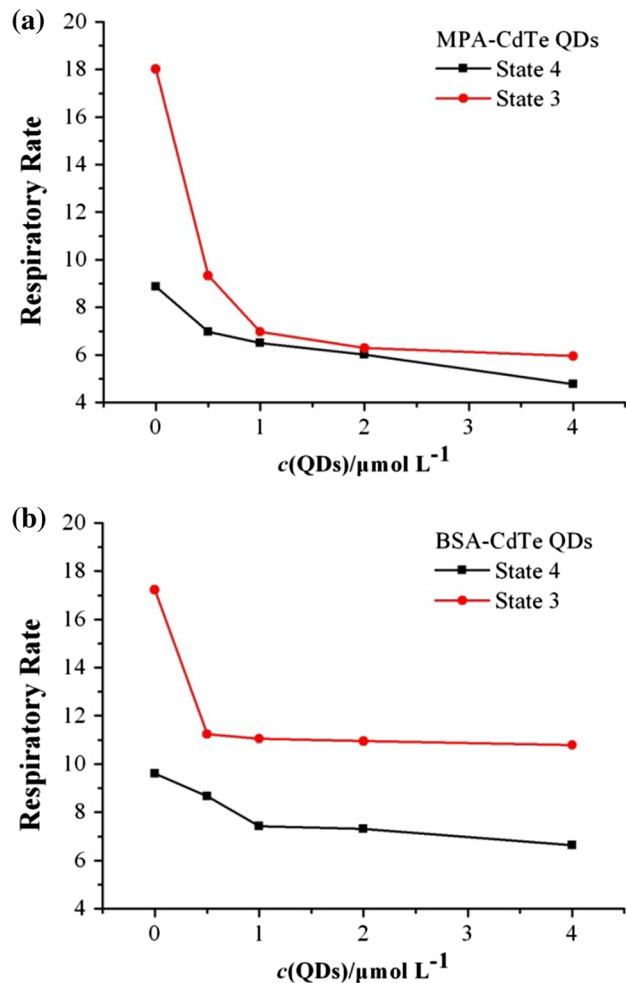


Fig. 10 Effects of QDs on the respiration of isolated mitochondria. Respiration unit represented as nanomole $\text{O}_2/\text{min}/\text{mg}$ protein. Respiratory rate was monitored by a Clark oxygen electrode. **a** Mitochondria followed by addition of MPA-CdTe QDs: 0, 1, 2, and 4 $\mu\text{mol L}^{-1}$. **b** Mitochondria followed by addition of BSA-CdTe QDs: 0, 1, 2, and 4 $\mu\text{mol L}^{-1}$. The respiratory rates at state 3 and state 4 significantly decreased with the increase of the QDs concentration. The traces are typical recordings representative of four experiments obtained from different mitochondrial preparations

enter cells via endocytosis and damage the plasma membrane, further leading to cell apoptosis (Han et al. 2012). Mitochondria, as the power source of the cell, is one of the key targets for QDs (Li et al. 2011a).

Herein, we first examined the toxicity of QDs on mitochondria at the level of cell by staining with JC-1 and transmission electron microscopy. The results showed that MPA-CdTe QDs caused a pronounced reduction of mitochondrial membrane potential (Figs. 3, 4). Moreover, the addition of MPA-CdTe QDs induced mitochondrial swelling with a large intermembrane space, clustering of the cristae, and expansion of the volume (Fig. 6). In order to obtain the direct and immediate influence of QDs on mitochondria, and further define the possible mechanisms of

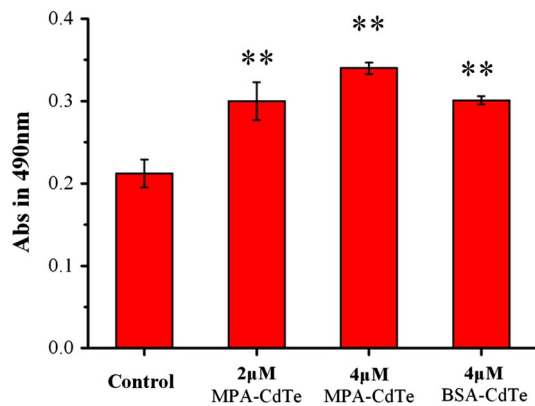


Fig. 11 Effects of QDs on the release of cytochrome *c* in the mitochondria. The concentration of cytochrome *c* is proportionate to absorbance at 490 nm. The average absorbance (mean \pm SE) statistically different from control (in the absence of MPA-CdTe QDs): ** $P < 0.01$ for ANOVA (paired *t* test). Error bars represent standard error of the mean

the interaction of QDs and mitochondria, we investigated the effects of CdTe QDs modified with different ligands on the function of mitochondria isolated from rat liver.

The mitochondrial permeability transition, or MPT, was defined as an increase in the permeability of the mitochondrial membranes to molecules of less than 1500 Da in molecular weight (Bernardi et al. 1992). MPT results from the opening of a mitochondrial permeability transition pore, also known as the MPT pore. The MPT pore was a protein pore that was formed in the inner membrane of the mitochondria under certain pathological conditions such as traumatic brain injury and stroke (Kobayashi et al. 2003). Induction of the permeability transition pore can lead to mitochondrial swelling, collapse of the transmembrane potential, and cell death through apoptosis or necrosis. For comparison, we examined the effects of MPA-CdTe QDs, BSA-CdTe QDs, and Cd^{2+} on MPT. Our data suggested that QDs induced MPT, which could be proved by the following experiments.

First, mitochondrial swelling, as a hallmark of mitochondrial dysfunction, is the direct results of the opening of the MPT pore (Gerencser et al. 2008; Liu et al. 2011). As shown in Fig. 5, CdTe QDs induced mitochondrial swelling. Mitochondrial swelling occurred as an osmotic result of the increase of mitochondrial matrix concentration, which caused water uptake (Passarella et al. 2003).

Second, as reported, there existed a strict correlation between changes of membrane fluidity and the increase of membrane permeability due to MPT induction (Passarella et al. 2003). The increase in membrane fluidity reflected a conformational change of pore-forming protein or proteins and potentiated the intrinsic proton permeability of the lipid bilayer, the so-called proton leak (Ricchelli et al.

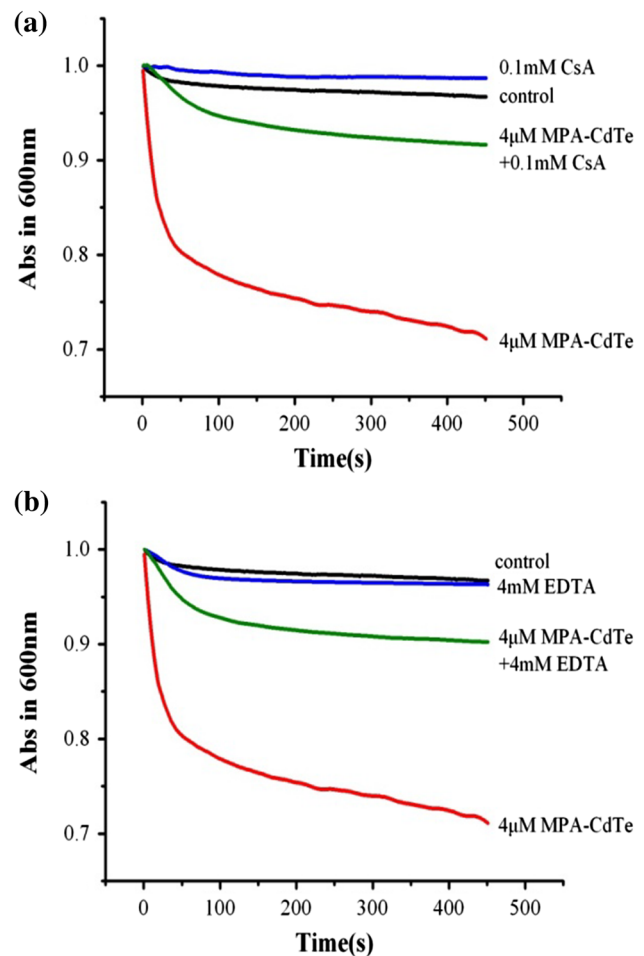


Fig. 12 Effects of CsA (a) and EDTA (b) on mitochondrial swelling induced by MPA-CdTe QDs. Isolated mitochondria (0.25 mg/mL) were suspended in 3 mL of buffer containing 200 mM sucrose, 10 mM Tris-MOPS, 20 μM EGTA-Tris, 5 mM succinate, 2 μM rotenone, and 3 $\mu\text{g/mL}$ oligomycin (pH 7.4). Mitochondria suspension incubated with different inhibitors (CsA and EDTA) before measuring. **a** The addition of 4 μM MPA-CdTe QDs led to mitochondrial swelling. CsA (0.1 mM) partially inhibited the swelling. **b** The addition of 4 μM MPA-CdTe QDs led to mitochondrial swelling. EDTA (4 mM) partially inhibited the swelling. The traces are typical recordings representative of four experiments obtained from different mitochondrial preparations

1999; Zhang et al. 2011). Therefore, QDs are capable of modulating the conformation of proteins that form the MPT pore, enhancing mitochondrial membrane fluidity, and inducing MPT.

Third, reduced energy metabolism has been linked to a decrease in the $\Delta\psi_m$ (Li et al. 2011a). MPT induction is also due to the dissipation of the difference in voltage across the inner mitochondrial membrane. The reduction of the $\Delta\psi_m$ and decreased ATP were necessary for the induction of the MPT (Isenberg and Klaunig 2000). Moreover, induction of the MPT produces a further collapse of the mitochondrial membrane potential ($\Delta\psi_m$) and uncoupling of the electron transport chain from ATP production

which promotes the opening of additional MPT pores (Li et al. 2012). Our data suggested that CdTe QDs caused depolarization of the membrane and injury of mitochondrial bioenergetics.

Fourth, the ultrastructure of mitochondria was changed by CdTe QDs. The addition of MPA-CdTe QDs caused mitochondrial swelling with a large intermembrane space, clustering of the cristae, and expansion of the volume.

Taking the above four aspects into account, we conclude that CdTe QDs can trigger MPT. Previous reports have suggested that the MPT also induces the release of specific proteins from the mitochondria, and triggers the nuclear pathology of apoptosis in various organs such as the liver and brain (Kobayashi et al. 2003). MPT opening has been widely assumed to underlie the release of cytochrome *c*. Figure 11 indicates that QDs induce translocation of cytochrome *c*, which is supposed to be one of the proteins triggering apoptosis, from mitochondria to the cytosol. The controlled release of mitochondrial cytochrome *c* represents a key step within the induction of apoptosis. Cytochrome *c* release from mitochondria results in a decrease in both mitochondrial ATP production and membrane potential.

In order to expatiate on the interaction mechanism, we also evaluated the protective effects of CsA and EDTA. Previous studies and preliminary experiments in our group demonstrated pretreatment with CsA is necessary to prevent the MPT in mitochondria isolated from liver (Halestrap et al. 1997). Figure 12a shows pretreatment with 0.1 mM CsA inhibited the QD-induced swelling. Therefore, the protective effect of CsA confirms that mitochondrial swelling primarily occurs as the result of MPT. Furthermore, it is well established that CsA can effectively inhibit the mitochondrial swelling, collapse of the membrane potential and increase of membrane fluidity induced by Ca^{2+} (Zhang et al. 2011). Consequently, we speculated that QDs may be able to induce MPT via a Ca^{2+} -dependent domain. Previous studies indicated the toxicity of quantum dots attribute to the release of Cd^{2+} . Since the crystal ionic radius of Cd^{2+} is close to that of Ca^{2+} , QDs may induced MPT through a Ca^{2+} -triggering site. Figure 12b indicated the addition of the chelator EDTA into the QDs-induced MPT medium obviously inhibited the mitochondrial swelling. These results confirm that Ca^{2+} -triggering sites are involved in QDs-induced MPT. However, we observed that the influences of QDs and Cd^{2+} on mitochondrial membrane fluidity were different (Fig. 9b), e.g., the increase of membrane fluidity was detected after the addition of QDs (Zhang et al. 2011), whereas the membrane fluidity decreased in the presence of 32 or 320 μM Cd^{2+} . Consequently, the release of Cd^{2+} is not the sole reason for the QDs-induced mitochondrial dysfunction. We speculate that the toxicity mechanism of QDs may be related to the nanoscale effect of QDs.

In order to stabilize QDs, alleviate toxicity and target organs, quantum dots are usually coated with ligands or polymers, or functionalized with peptide sequences. Because the surface coating molecules play a dominant role in the biomedical applications of quantum dots, the influences of ligands on the toxicity of quantum dots should be investigated in detail so that their potential risks to human and the environment can be fully elucidated. Reportedly, the presence of BSA greatly improved the biocompatibility of QDs at the level of cells. We wonder if BSA has the same effect at the level of organelle. To this end, we prepared two types of CdTe quantum dots with nearly identical maximum emission wavelength but capped with MPA and BSA, respectively. The binding of BSA on the surface of QDs can alleviate the release of Cd^{2+} . Compared with MPA-CdTe QDs, however, BSA-CdTe QDs had a greater effect on the mitochondrial swelling, membrane fluidity, and permeabilization to H^+ and K^+ by mitochondrial inner membrane. It may be attributed to the fact that BSA is more lipophilic than MPA. Besides, it further confirms that the release of Cd^{2+} is not the sole reason for QDs-induced mitochondrial dysfunction.

Conclusion

This work presents the effects of CdTe QDs modified with different ligands on MPT. The results showed that QDs induced MPT, which resulted in mitochondrial swelling, collapse of the membrane potential, inner membrane permeability to H^+ and K^+ , the increase of membrane fluidity, depression of respiration, alterations of ultrastructure, and release of cytochrome *c*. Furthermore, the protective effect of CsA and EDTA confirmed that QDs were able to induce MPT via a Ca^{2+} -dependent domain. Noteworthy, the influences of QDs and Cd^{2+} on mitochondrial membrane fluidity were different. Compared with MPA-CdTe QDs, BSA-CdTe QDs had a greater effect on the mitochondrial swelling, membrane fluidity, and permeabilization to H^+ and K^+ by mitochondrial inner membrane, due to the greater lipophilicity of BSA than MPA. In conclusion, our study provides an important basis for understanding the mechanism of toxicity of CdTe QDs to mitochondria. The procedures here will be highly useful for evaluation of the safety of QDs.

Acknowledgments The authors gratefully acknowledge the financial support from Chinese 973 Program (Grant No. 2011CB933600), National Science Fund for Distinguished Young Scholars of China (Grant No. 21225313), Educational Commission of Hubei Province of China (Grant No. Q20141302), National Natural Science Foundation of China (Grant Nos. 21403017, 21303126), Large-scale Instrument And Equipment Sharing Foundation of Wuhan University and Fundamental Research Funds for the Central Universities.

References

- Atay Z, Biver T, Corti A, Eltugral N, Lorenzini E, Masini M, Paolicchi A, Pucci A, Ruggeri G, Secco F, Venturini M (2010) Non-covalent interactions of cadmium sulphide and gold nanoparticles with DNA. *J Nanopart Res* 12:2241–2253
- Bernardi P, Vassanelli S, Veronese P, Colonna R, Szabo I, Zoratti M (1992) Modulation of the mitochondrial permeability transition pore. Effect of protons and divalent cations. *J Biol Chem* 267:2934–2939
- Bernardi P, Broekemeier KM, Pfeiffer DR (1994) Recent progress on regulation of the mitochondrial permeability transition pore; a cyclosporin-sensitive pore in the inner mitochondrial membrane. *J Bioenerg Biomembr* 26:509–517
- Chan WH, Shiao NH, Lu PZ (2006) CdSe quantum dots induce apoptosis in human neuroblastoma cells via mitochondrial-dependent pathways and inhibition of survival signals. *Toxicol Lett* 167:191–200
- Chibli H, Carlini L, Park S, Dimitrijevic NM, Nadeau JL (2011) Cytotoxicity of InP/ZnS quantum dots related to reactive oxygen species generation. *Nanoscale* 3:2552–2559
- Clift MJ, Brandenberger C, Rothen-Rutishauser B, Brown DM, Stone V (2011a) The uptake and intracellular fate of a series of different surface coated quantum dots in vitro. *Toxicology* 286: 58–68
- Clift MJ, Varet J, Hankin SM, Brownlee B, Davidson AM, Brandenberger C, Rothen-Rutishauser B, Brown DM, Stone V (2011b) Quantum dot cytotoxicity in vitro: an investigation into the cytotoxic effects of a series of different surface chemistries and their core/shell materials. *Nanotoxicology* 5:664–674
- Deckwerth TL, Johnson EM (1993) Temporal analysis of events associated with programmed cell death (apoptosis) of sympathetic neurons deprived of nerve growth factor. *J Cell Biol* 123:1207–1222
- Derfus AM, Chan WCW, Bhatia SN (2004) Probing the cytotoxicity of semiconductor quantum dots. *Nano Lett* 4:11–18
- Donaldson K, Brown D, Clouter A, Duffin R, MacNee W, Renwick L, Tran L, Stone V (2002) The pulmonary toxicology of ultrafine particles. *J Aerosol Med* 15:213–220
- Ekimov A, Onushchenko A (1981) Quantum size effect in three-dimensional microscopic semiconductor crystals. *ZhETF Pis ma Redaktsiiu* 34:363
- Fernandes MA, Custódio J, Santos MS, Moreno AJ, Vicente JA (2006) Tetrandrine concentrations not affecting oxidative phosphorylation protect rat liver mitochondria from oxidative stress. *Mitochondrion* 6:176–185
- Freyre-Fonseca V, Delgado-Buenrostro NL, Gutiérrez-Cirlos EB, Calderón-Torres CM, Cabellos-Avelar T, Sánchez-Pérez Y, Pinzón E, Torres I, Molina-Jijón E, Zazueta C (2011) Titanium dioxide nanoparticles impair lung mitochondrial function. *Toxicol Lett* 202:111–119
- Gerencser AA, Doczi J, Töröcsik B, Bossy-Wetzel E, Adam-Vizi V (2008) Mitochondrial swelling measurement in situ by optimized spatial filtering: astrocyte-neuron differences. *Biophys J* 95: 2583–2598
- Halestrap A, Connern C, Griffiths E, Kerr P (1997) Cyclosporin A binding to mitochondrial cyclophilin inhibits the permeability transition pore and protects hearts from ischaemia/reperfusion injury. In *Detection of mitochondrial diseases*. Springer, New York, pp 167–172
- Han X, Lai L, Tian F, Jiang FL, Xiao Q, Li Y, Yu Q, Li D, Wang J, Zhang Q (2012) Toxicity of CdTe quantum dots on yeast *Saccharomyces cerevisiae*. *Small* 8:2680–2689
- Henze K, Martin W (2003) Evolutionary biology: essence of mitochondria. *Nature* 426:127–128
- Hoshino A, Fujioka K, Oku T, Suga M, Sasaki YF, Ohta T, Yasuhara M, Suzuki K, Yamamoto K (2004) Physicochemical properties and cellular toxicity of nanocrystal quantum dots depend on their surface modification. *Nano Lett* 4:2163–2169
- Isenberg JS, Klaunig JE (2000) Role of the mitochondrial membrane permeability transition (MPT) in rotenone-induced apoptosis in liver cells. *Toxicol Sci* 53:340–351
- Kobayashi T, Kuroda S, Tada M, Houkin K, Iwasaki Y, Abe H (2003) Calcium-induced mitochondrial swelling and cytochrome *c* release in the brain: its biochemical characteristics and implication in ischemic neuronal injury. *Brain Res* 960:62–70
- Lesnefsky EJ, Moghaddas S, Tandler B, Kerner J, Hoppel CL (2001) Mitochondrial dysfunction in cardiac disease: ischemia-reperfusion, aging, and heart failure. *J Mol Cell Cardiol* 33:1065–1089
- Leutwyler WK, Bürgi SL, Burgli H (1996) Semiconductor clusters, nanocrystals, and quantum dots. *Science* 271:933
- Li J, Zhang Y, Xiao Q, Tian F, Liu X, Li R, Zhao G, Jiang F, Liu Y (2011a) Mitochondria as target of quantum dots toxicity. *J Hazard Mater* 194:440–444
- Li JH, Zhang Y, Xiao Q, Tian FF, Liu XR, Li R, Zhao GY, Jiang FL, Liu Y (2011b) Mitochondria as target of quantum dots toxicity. *J Hazard Mater* 194:440–444
- Li JH, Liu XR, Zhang Y, Tian FF, Zhao GY, Jiang FL, Liu Y (2012) Toxicity of nano zinc oxide to mitochondria. *Toxicol Res* 1:137–144
- Liu XR, Li JH, Zhang Y, Ge YS, Tian FF, Dai J, Jiang FL, Liu Y (2011) Mitochondrial permeability transition induced by different concentrations of zinc. *J Membr Biol* 244:105–112
- Loss D, DiVincenzo DP (1998) Quantum computation with quantum dots. *Phys Rev A* 57:120
- Lovrić J, Cho SJ, Winnik FM, Maysinger D (2005) Unmodified cadmium telluride quantum dots induce reactive oxygen species formation leading to multiple organelle damage and cell death. *Chem Biol* 12:1227–1234
- Lu ZS, Li CM, Bao HF, Qiao Y, Toh YH, Yang X (2008) Mechanism of antimicrobial activity of CdTe quantum dots. *Langmuir* 24:5445–5452
- McBride HM, Neuspil M, Wasiak S (2006) Mitochondria: more than just a powerhouse. *Curr Biol* 16:R551–R560
- Michalet X, Pinaud F, Bentolila L, Tsay J, Doose S, Li J, Sundaresan G, Wu A, Gambhir S, Weiss S (2005) Quantum dots for live cells, in vivo imaging, and diagnostics. *Science* 307:538–544
- Mortensen LJ, Jatana S, Gelein R, De Benedetto A, de Mesy Bentley KL, Beck LA, Elder A, DeLouise LA (2013) Quantification of quantum dot murine skin penetration with UVR barrier impairment. *Nanotoxicology* 7:1386–1398
- Murray CB, Kagan C, Bawendi M (2000) Synthesis and characterization of monodisperse nanocrystals and close-packed nanocrystal assemblies. *Annu Rev Mater Sci* 30:545–610
- Narukawa Y, Kawakami Y, Funato M, Fujita S, Fujita S, Nakamura S (1997) Role of self-formed InGaN quantum dots for exciton localization in the purple laser diode emitting at 420 nm. *Appl Phys Lett* 70:981–983
- Neibert KD, Maysinger D (2012) Mechanisms of cellular adaptation to quantum dots—the role of glutathione and transcription factor EB. *Nanotoxicology* 6:249–262
- Nozik A (2002) Quantum dot solar cells. *Phys E* 14:115–120
- Passarella S, Atlante A, Valenti D, de Bari L (2003) The role of mitochondrial transport in energy metabolism. *Mitochondrion* 2:319–343
- Petronilli V, Šileikytė J, Zulian A, Dabbeni-Sala F, Jori G, Gobbo S, Tognon G, Nikolov P, Bernardi P, Ricchelli F (2009) Switch from inhibition to activation of the mitochondrial permeability transition during hematoporphyrin-mediated photooxidative

- stress: unmasking pore-regulating external thiols. *Biochim Biophys Acta (BBA) Bioenerg* 1787:897–904
- Pulskamp K, Diabaté S, Krug HF (2007) Carbon nanotubes show no sign of acute toxicity but induce intracellular reactive oxygen species in dependence on contaminants. *Toxicol Lett* 168:58–74
- Ricchelli F, Gobbo S, Moreno G, Salet C (1999) Changes of the fluidity of mitochondrial membranes induced by the permeability transition. *Biochemistry* 38:9295–9300
- Ricchelli F, Jori G, Gobbo S, Nikolov P, Petronilli V (2005) Discrimination between two steps in the mitochondrial permeability transition process. *Int J Biochem Cell Biol* 37:1858–1868
- Smiley ST, Reers M, Mottola-Hartshorn C, Lin M, Chen A, Smith TW, Steele GD, Chen LB (1991) Intracellular heterogeneity in mitochondrial membrane potentials revealed by a J-aggregate-forming lipophilic cation JC-1. *Proc Natl Acad Sci* 88:3671–3675
- Stensberg MC, Madangopal R, Yale G, Wei Q, Ochoa-Acuña H, Wei A, Mclamore ES, Rickus J, Porterfield DM, Sepúlveda MS (2014) Silver nanoparticle-specific mitotoxicity in *Daphnia magna*. *Nanotoxicology* 8:833–842
- Sun L, Li Y, Liu X, Jin M, Zhang L, Du Z, Guo C, Huang P, Sun Z (2011) Cytotoxicity and mitochondrial damage caused by silica nanoparticles. *Toxicol In Vitro* 25:1619–1629
- Teodoro JS, Simões AM, Duarte FV, Rolo AP, Murdoch RC, Hussain SM, Palmeira CM (2011) Assessment of the toxicity of silver nanoparticles in vitro: a mitochondrial perspective. *Toxicol In Vitro* 25:664–670
- Vannoy CH, Leblanc RM (2010) Effects of DHLA-capped CdSe/ZnS quantum dots on the fibrillation of human serum albumin. *J Phys Chem B* 114:10881–10888
- Werlin R, Priester JH, Mielke RE, Kramer S, Jackson S, Stoimenov PK, Stucky GD, Cherr GN, Orias E, Holden PA (2011) Biomagnification of cadmium selenide quantum dots in a simple experimental microbial food chain. *Nat Nanotechnol* 6:65–71
- Xiao J, Kai G, Chen X (2012) Effect of CdTe QDs on the protein-drug interactions. *Nanotoxicology* 6:304–314
- Yang Y, Lan J, Xu Z, Chen T, Zhao T, Cheng T, Shen J, Lv S, Zhang H (2014) Toxicity and biodistribution of aqueous synthesized ZnS and ZnO quantum dots in mice. *Nanotoxicology* 8:107–116
- Zamzami N, Marchetti P, Castedo M, Hirsch T, Susin SA, Masse B, Kroemer G (1996) Inhibitors of permeability transition interfere with the disruption of the mitochondrial transmembrane potential during apoptosis. *FEBS Lett* 384:53–57
- Zhang Y, Li JH, Liu XR, Jiang FL, Tian FF, Liu Y (2011) Spectroscopic and microscopic studies on the mechanisms of mitochondrial toxicity induced by different concentrations of cadmium. *J Membr Biol* 241:39–49
- Zheng Y, Gao S, Ying JY (2007) Synthesis and cell-imaging applications of glutathione-capped CdTe quantum dots. *Adv Mater* 19:376–380